

FINITE ELEMENT SIMULATION OF INCOMPRESSIBLE FLOW WITH MOVING BOUNDARIES

M. S. ENGELMAN

(Fluid Dynamics International, 1600 Orrington Avenue, Evanston, IL 60201)

Introduction

Flows involving a moving fluid interface are often encountered in many scientific and engineering applications. Extrusion of liquids, problems in capillarity, crystal growth, electrochemical plating and corrosion, metal and glass forming processes, and the coating of solid substrates with liquids are examples of such flows. If the interface is between a gas and a liquid, it is frequently referred to as a free surface.

Computer aided analysis can play a significant role in understanding, operating and controlling such processes in both laboratory and industrial settings. It would enable the analyst/engineer to perform simulations and parametric studies to determine the system configuration and characteristics subject to various different flow rates, temperature profiles, etc. on the computer rather than in the laboratory, and in many instances greatly improve and shorten the design process. To carry out such analyses requires a technique which can accurately represent system variables on a deforming, irregular domain whose free surface portions may be unknown a priori. The Galerkin-finite element technique has aspects which suit it well to such irregular and possible time dependent domain problems since, for example, it can easily accommodate the higher resolution required in certain regions, the singularities associated with contact lines and the complicated boundary conditions associated with such system. The basic approach to problems involving a free surface presented herein involves a deforming spatial mesh where nodes located on a free surface are allowed to move such that they remain on the free surface. An additional degree of freedom is associated with the nodes on the free surface which directly determines their location in space. This is then coupled with a Newton-type iterative procedure which results in the simultaneous calculation of the position of the nodes on the free surface and the field variables at the new nodal positions once convergence is attained.

2. Formulation of the Continuum Problem

The equations of incompressible fluid flow are derived from the basic physical principles of conservation of mass and linear momentum and are the well-known Navier-Stokes equations. The equations for a free surface flow problem are identical except that the location of the free surface is unknown and is determined by additional boundary conditions at the free surface. In the numerical procedure the nodes on the free surface are allowed to move. This requires the addition of a new degree of freedom to the problem to account for the changing shape of the fluid mass.

At a free surface, continuity of stress and velocity is required which leads to the conditions,

$$u_n = 0, \quad x \in \Gamma_f, \quad (1a)$$

$$f_n - p_0 = 2\sigma H, \quad x \in \Gamma_f, \quad (1b)$$

$$f_t = 0, \quad x \in \Gamma_f, \quad (1c)$$

where $u_n = u_i n_i$ is the normal component of velocity, $f_n = \sigma_{ij} n_j n_i$ the normal, and $f_t = \sigma_{ij} n_j t_i$ the tangential component of the stress vector at the boundary, σ is the surface tension, p_0 the pressure in the adjacent vapor phase and H the mean Gaussian curvature of the surface. These conditions can also be written in dimensionless form as:

$$\begin{aligned} u_n &= 0, \\ f_n &= p_0 + \frac{1}{\text{Re} \cdot \text{Ca}} 2H, \\ f_t &= 0, \end{aligned} \quad (2)$$

where u_i, p, p_0 are dimensionless quantities and $\text{Ca} = \mu U / \sigma$ is the capillary number.

In the general three-dimensional case, the mean Gaussian curvature of a surface H is equal to $\frac{1}{2}(K_1 + K_2)$, where K_1 and K_2 are the principal curvatures of a surface. It is not necessary to choose the principal curvatures, however it is often more convenient to do so. In the two-dimensional case, the curvature of a "surface" reduces to the curvature of a line with one of the principal curvatures, K_2 , being zero. For a line, the curvature vector is,

$$k = Kn = (\nabla \cdot n)n = -\frac{dt}{ds}$$

where n is the normal vector to the line and t is the tangent vector, i.e. the curvature is equal to the change in the tangent vector as one moves along the line.

3. Finite Element Formulation

Since the details of application of the FEM to the basic equations of fluid flow can be found elsewhere [1], this section will concentrate only on those aspects of the procedure introduced as a result of the free surface. At each node on the free surface a new degree of freedom is introduced; the value of this degree of freedom will enable the determination of the position of the node within the region and is

an integral part of the representation of the free surface. This degree of freedom must be chosen so that it is easily incorporated into the equations describing the fluid motion, as well as constraining the motion of the node so as to avoid greatly deformed meshes. The technique for representing the free surface degree of freedom is a generalization of the method developed by Saito and Scriven [2], where nodes in the mesh which are free to move lie on generator lines called spines. Referring to Figure 1, a node's position is represented parametrically as:

$$\begin{aligned}x_i &= \alpha_x[h_{j+1} + \omega t_i(h_j - h_{j+1})] + \beta_x, \\y_i &= \alpha_y[h_{j+1} + \omega t_i(h_j - h_{j+1})] + \beta_y, \\z_i &= \alpha_z[h_{j+1} + \omega t_i(h_j - h_{j+1})] + \beta_z,\end{aligned}\tag{3}$$

where h_j is the interface location parameter for a given spine, $\alpha = (\alpha_x, \alpha_y, \alpha_z)$ is the direction vector, and $\beta = (\beta_x, \beta_y, \beta_z)$ is the base point of the spine. The location (x_i, y_i, z_i) of a node on the spine which is free to move is determined from its relative position, ωt_i , to the moving interfaces located at h_j and h_{j+1} .

This parametric approach allows the initial aspect ratio of the nodes on a spine to be easily maintained as each node on a spine will retain the same relative position between the interfaces. Also note that each of the spines is independent of the other spines. The interface location parameters, h_j , are the new degrees of freedom introduced.

Inputting the spine and interface location information requires relatively little additional input; primarily the list of nodes that comprise the generator lines. Nodes lying on the generator lines are considered free to move; points not located on spines are fixed mesh points. As a result of the parametric representation used for the location of a node, nodes located between moving interfaces will retain the same aspect ratio as set up by initial mesh. In the event that there is only one free surface, the second interface is assumed to be a fixed reference interface located at the last node of the spine. This artificial reference interface does not add any additional degrees of freedom to the system.

In the finite element context, the free surface consists of a collection of line segments of N nodes each, where N depends on the order of the approximation used. The coordinates of a point on one of these line segments can be represented by:

$$\begin{aligned}x &= \sum x_i \chi_i(s) = \sum (\alpha_x h_{j,i} + \beta_x) \chi_i(s), \\y &= \sum y_i \chi_i(s) = \sum (\alpha_y h_{j,i} + \beta_y) \chi_i(s), \\z &= \sum z_i \chi_i(s) = \sum (\alpha_z h_{j,i} + \beta_z) \chi_i(s),\end{aligned}\tag{4}$$

where $\chi_i(s)$ is the basis function used to approximate the free surface line segments.

The Galerkin finite element method can now be applied to the equations of fluid motion and the free surface boundary conditions. This results in a matrix system of nonlinear algebraic equations of the form:

$$\begin{aligned}M\dot{U} + A(U)U + K(T, U)U - CP + BX &= F, \\C^T U &= 0, \\K_n U &= 0,\end{aligned}\tag{5}$$

where X is the global vector of the free surface unknowns, $A(U)$ is a matrix which represents the contribution from the convective terms, $K(U)$ is a matrix which includes the diffusive terms, C is the divergence matrix, B is the matrix representing the contribution of the normal stress balance boundary condition in the momentum equation, K_n contains the normal velocity boundary condition effects and F is a vector including the effects of the body force, applied tractions and contact angle boundary conditions.

4. Solution of the Finite Element Equations

It now remains to solve the nonlinear system of equations (5). A fixed point iterative procedure could be used, however, this would necessitate the interpolation of the nodal velocity degrees of freedom to the new nodal positions at each iteration; such a method would also exhibit a linear rate of convergence. On the other hand, if a Newton-type method, e. g. Newton-Raphson or quasi-Newton, is utilized and complete account of the variation with respect to the free surface degrees of freedom is incorporated into the system Jacobian, then at the end of each iteration the velocity solution will represent the velocities at the new nodal location. The great advantage of this approach is that the free surface location and the velocities at the new nodal locations are a direct result of the iterative procedure with no interpolation or updating being required.

Solving the global system of FEM equations using the Newton-Raphson or quasi-Newton method requires the determination of the Jacobian matrix of equations (5). This Jacobian matrix is defined by:

$$J(u) = \frac{\partial R(u)}{\partial u} \quad (6)$$

where $u = u(u_i, p, T, x)$ is the solution vector and $R(u)$ is the residual vector for the system (5).

The evaluation of the Jacobian $J(u)$ is particularly tedious as the matrices K , A , N and K_n and the vector F depend on X (or rather x and y) by equations (3), not only through the integrands, but also through the limits of integration, i.e. the element domain. However, just as the integrals over fixed elements are handled by mapping an element onto a 'parent' or reference element and performing the integration over its simpler, fixed geometry, the same technique can be used to compute the variation of the various matrices with respect to X (see [3] for complete details). The line integrals which arise from the boundary conditions on the free surface also contribute to the global Jacobian matrix. The variation of these boundary line integrals with respect to the free surface degrees of freedom X can again be computed by making use of the isoparametric mapping concept.

5. Time Dependent Problems

The technique for handling the free surface movement for a transient free surface problem is identical to that described for steady state problems. Care, however, must be taken in the treatment of the time derivatives which now appear in the momentum equations and the free surface boundary condition.

The momentum equation for a transient flow is,

$$\rho \left(\frac{\partial u_i}{\partial t} + u_j u_{i,j} \right) = \sigma_{ij,j} + \rho b_i. \quad (7)$$

Also the condition of no normal flow across the free surface, equation (1a), must be modified to,

$$\frac{\partial S}{\partial t} + \mathbf{u} \cdot \nabla S = 0 \quad (8)$$

where $S(x, y, t) = 0$ is the function defining the free surface. If this equation is normalized by dividing by $|\nabla S|$, it becomes,

$$\frac{\partial \bar{S}}{\partial t} + \mathbf{u} \cdot \mathbf{n} = 0 \quad ; \quad \bar{S} = \frac{S}{|\nabla S|}. \quad (9)$$

The time derivatives appearing in equations (7) and (9) are Eulerian time derivatives, i.e. the nodal velocity field must be for nodes fixed in space. However, the technique of parameterization of the free surface is such that the nodes are not fixed in some frame of reference (Eulerian formulation), nor are they fixed in a frame of reference carried along by the fluid (Lagrangian formulation); rather each node is constrained to move along a fixed line in space - a mixed Eulerian-Lagrangian formulation. Thus the time derivatives in equations (7) and (9) must be transformed to time derivatives which follow the moving nodes along these lines.

Denoting by $\delta/\delta t$ the time derivative following a moving node, the relationship between $\delta/\delta t$ and $\partial/\partial t$, the Eulerian time derivative is given by,

$$\begin{aligned} \frac{\delta}{\delta t} &= \frac{\partial}{\partial t} + \frac{\partial \mathbf{x}}{\partial t} \cdot \nabla \\ &= \frac{\partial}{\partial t} + \frac{\delta \bar{S}}{\delta t} \frac{\partial \mathbf{x}}{\partial \bar{S}} \cdot \nabla. \end{aligned} \quad (10)$$

where $\mathbf{x} = \mathbf{x}(\bar{S}, \xi, \eta)$ are the coordinates of a moving nodal point. The finite element implementation follows in the standard fashion. The time derivatives are discretized in the usual manner using a finite difference scheme (refer to Gresho et. al. [4] for complete details on the time integration scheme).

6. Temperature Dependent Problems

Many free surface flows of interest possess not only flow but concomitant heat transport which, combined with presence of a free surface, can lead to a significant

“surface tension driven” flow contribution. This is often referred to as Marangoni convection, or thermocapillary convection when a distinction is to be made in the case of temperature-induced surface tension variations.

The techniques outlined in the previous sections are directly extendible to such flows. Temperature dependence is introduced in an identical manner to that described in the previous chapters. The only modification in the free surface boundary condition is that equation (1c) is modified to,

$$f_t = \nabla_s \sigma \quad , \quad x \in \Gamma \quad (11)$$

in order to account for temperature-induced variations in the surface tension.

7. Numerical Simulations

Two numerical simulations are presented in this section to illustrate the algorithm outlines in the paper. The first example is the evolution of a drop from a nozzle. The motion of the fluid is driven by the prescribed movement of a rigid piston. This forces an efflux of liquid from a small aperture at a rate determined by mass conservation. This example illustrates the simulation of both a moving boundary, the piston, and the free surface of the drop. The operation of an ink-jet printer is very similar to this problem where the piston is usually an electrically activated crystal. Figure 2 shows the evolution of the drop and the accompanying movement of the drop surface position superimposed at successive time steps. The drop tends to be spheroidal because of the absence of gravity-in the simulation.

The term roll coating covers a wide variety of processes used to coat a moving substrate. Fluid is taken up from a bath by a roller which dips into it, and then transferred, possibly through a trail of rollers onto a web. In this example, the flow between two adjacent rollers counterrotating at different speeds is modeled. Primary interest is focused as the free surface formed by the coating material as the rollers rotate. The free surface shape is determined by the roller speeds, their radii, the gap thickness and the physical properties of the liquid. In the present case, the rollers have radii 100 units and the gap width is 2 units. The speeds are in the ratio 2 : 1.

The results are shown in Figures 3–5. Figure 3 shows the superposition of the computed free surface shape and the initial guess. Note the asymmetry in the final free surface shape; this is due to the difference in roller speeds. Figures 4 and 5 show respectively, the velocity vectors and the streamlines of the flow. The latter illustrates the presence of a weak recirculation zone near the free surface. The inlet flow is a linear shear profile, while at the ends of the roller films the velocities are nearly constant.

References

- [1] M. S. Engelman, FIDAP Theoretical Manual, Fluid Dynamics International, November 1987.
- [2] H. Saito , L. E. Scriven, Study of coating flow by the finite element method, *J. Comp. phys.*, **42**, 53, 1981.
- [3] M. S. Engelman, R. L. Sani, Finite Element Simulation of Incompressible Flows with a Free/Moving Surface, in *Numerical Methods in Laminar and Turbulent Flow*, Pineridge Press, UK, 1984.
- [4] P. M. Gresho, R. L. Lee, R.L. Sani, On time dependent solution of the incompressible Navier-Stokes equations in two and three dimensions, *Recent Advances in Numerical Methods in Fluids*, Pineridge Press, Swansea, UK, 1980.

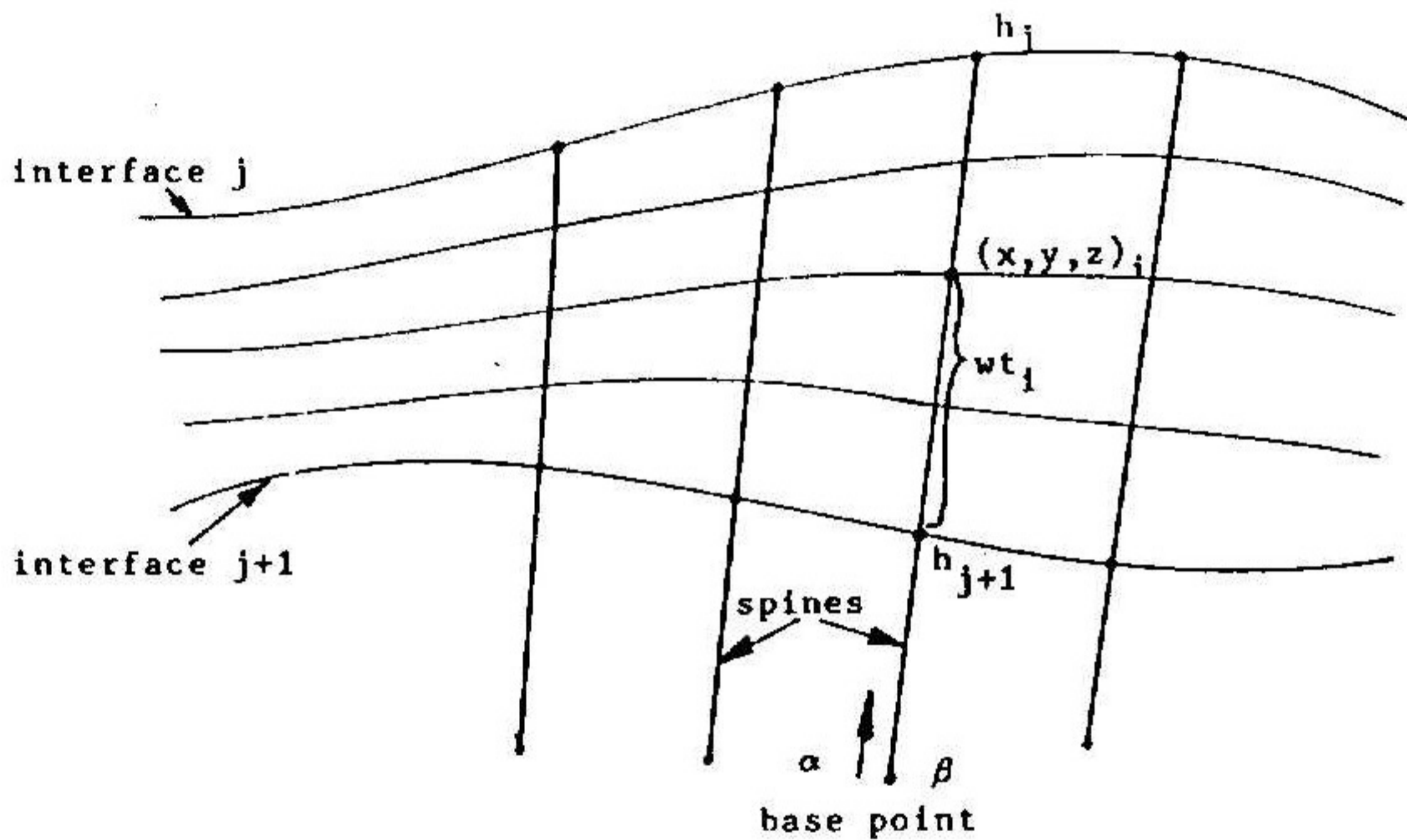


Fig. 1. Moving node position definition

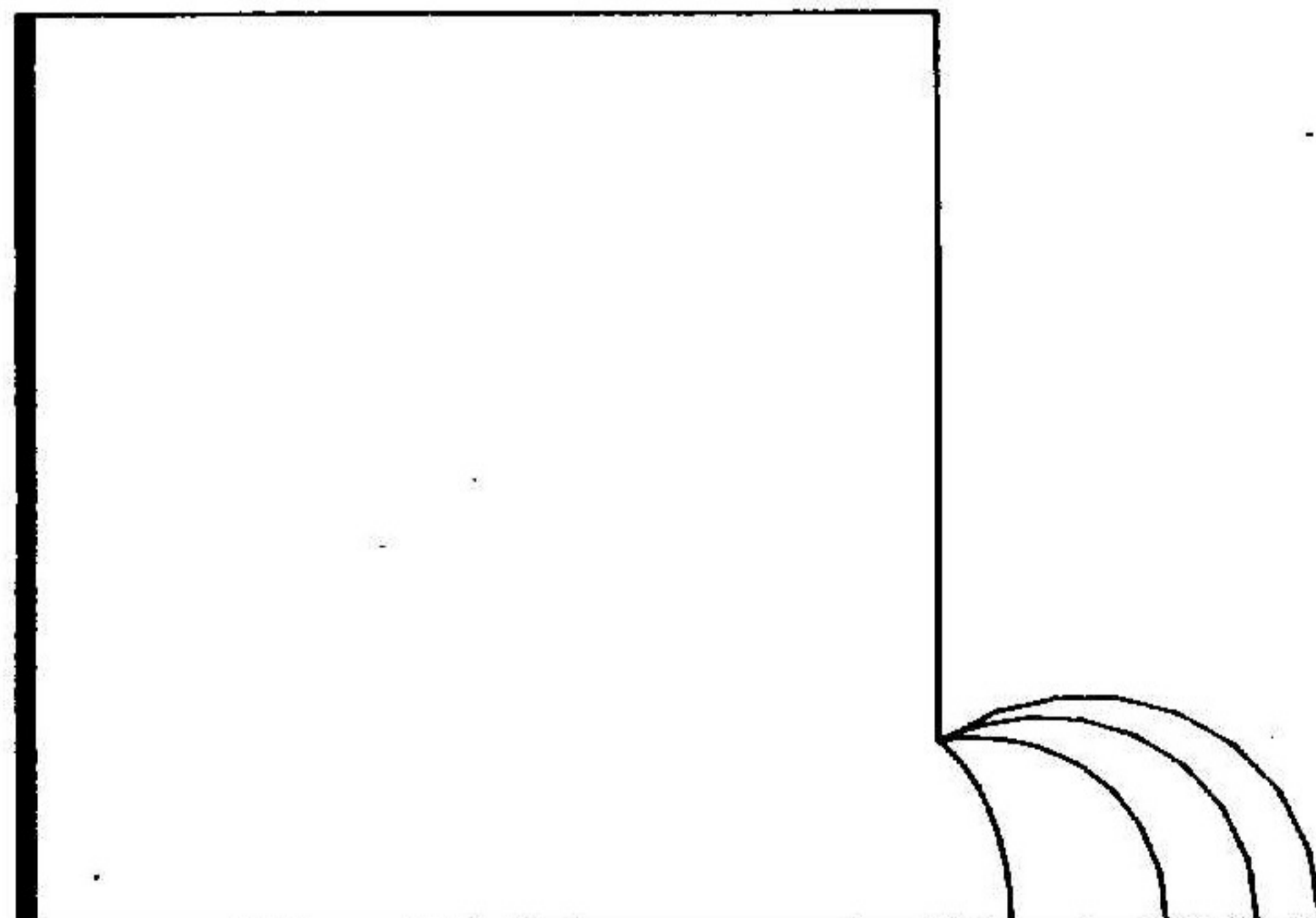


Fig. 2. Mesh configuration at successive time steps

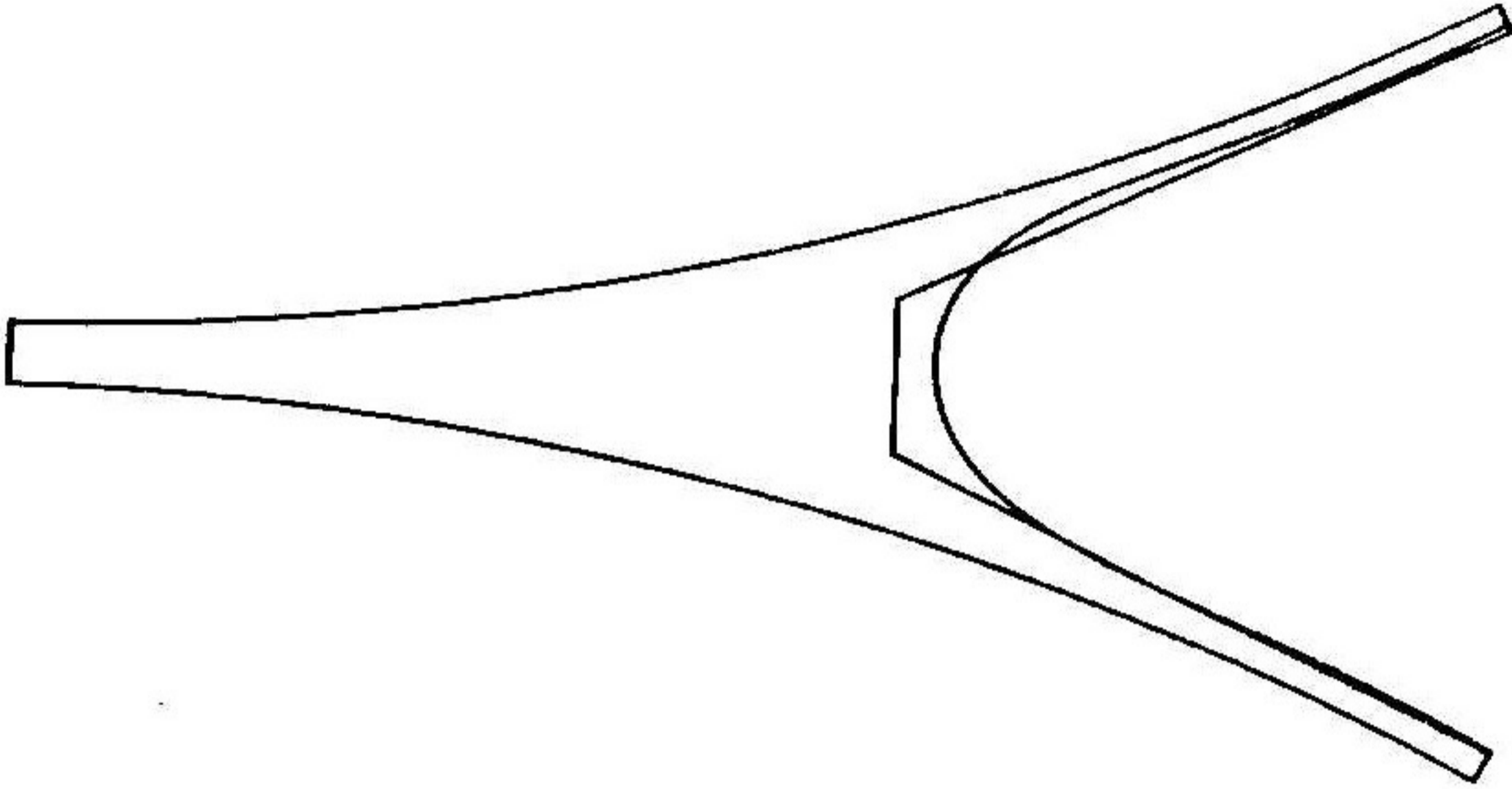


Fig. 3. Mesh deformation for double roll coater

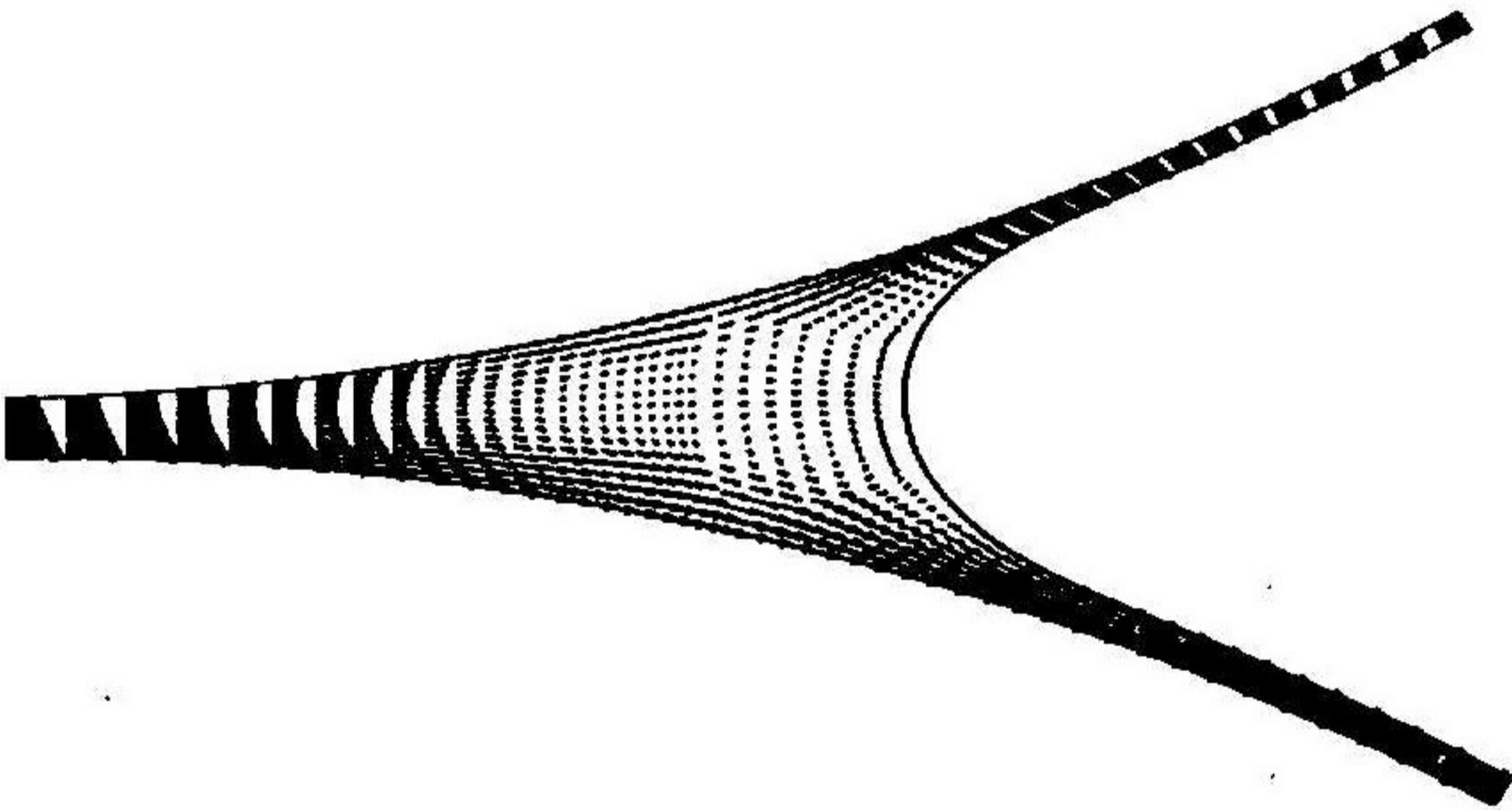


Fig. 4. Velocity vector plot double roll coater

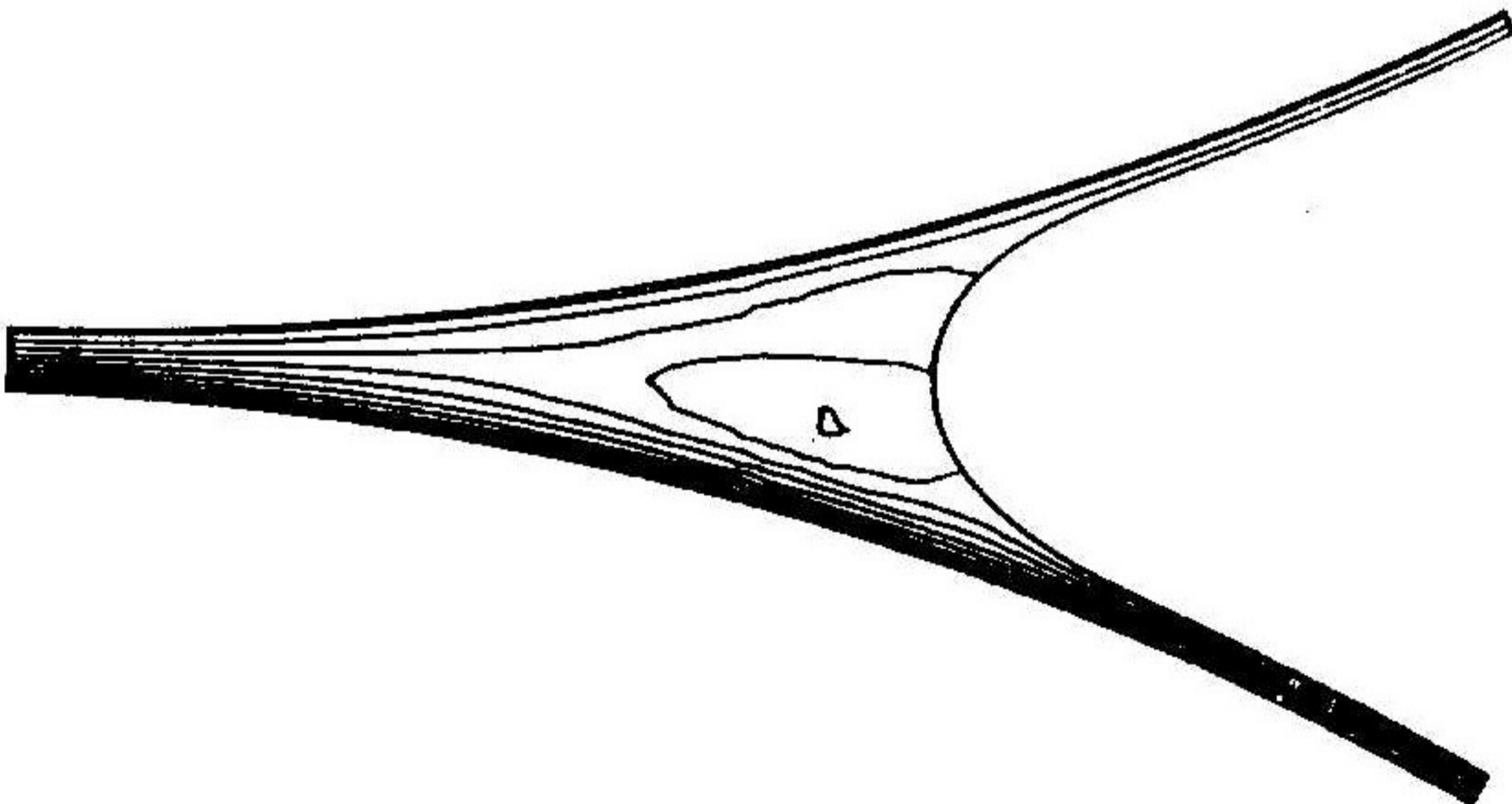


Fig. 5. Streamline contour plot for double roll coater